

# Colourimetric Carboxylate Anion Sensors Derived from Viologen-Based Receptors

Adam N. Swinburne,<sup>[a]</sup> Martin J. Paterson,<sup>[b]</sup> Kathrin H. Fischer,<sup>[a]</sup> Sara Jane Dickson,<sup>[a]</sup>  
Emma V. B. Wallace,<sup>[a]</sup> Warwick J. Belcher,<sup>[c]</sup> Andrew Beeby,\*<sup>[a]</sup> and  
Jonathan W. Steed\*<sup>[a]</sup>

**Abstract:** A series of tri- and tetrapodal viologen-based anion receptors showing a colourimetric response to carboxylates, such as acetate, have been synthesised. Alteration of the anion binding sites allows for binding site competition within a receptor. This results in a delayed colourimetric response for urea derivatives compared

with pyridinium systems because the anions are initially bound to the periphery of the receptor, away from the viologen unit. DFT calculations and ex-

perimental measurements allow the colour change to be assigned to an anion–receptor charge-transfer process, facilitated by the exceptionally low reduction potential of the cationic host compounds. Evidence for electron transfer to give the viologen radical cation is also seen in some cases.

**Keywords:** anions • charge transfer • cyclic voltammetry • density functional calculations • sensors

## Introduction

The design of anion receptors capable of selectively sensing an anion is a topical challenge.<sup>[1–4]</sup> Carboxylate recognition is of particular importance due to the variety of geometries, high basicity and biochemical importance of the anions. Although carboxylates bind strongly to hydrogen-bond donors, their basicity can also lead to deprotonation and decomposition.<sup>[5–7]</sup> The approach of our group<sup>[8–10]</sup> and others<sup>[11–14]</sup> is to use an induced-fit binding strategy based upon designing conformationally flexible anion receptors, typically derived

from a hexasubstituted triethylbenzene core. As the conformation of the host changes upon anion binding a fluorescent or electrochemical response is obtained.

A hexasubstituted triethylbenzene core has been used extensively as a scaffold for conformationally flexible receptors. Steric hindrance between adjacent ethyl and binding groups gives a 10–15 kcal mol<sup>−1</sup> preference to a “three-up, three-down” conformation.<sup>[15–17]</sup> This provides a degree of binding cavity preorganisation while still allowing flexibility. Binding and reporter groups can then be added in a modular approach to receptor design.<sup>[15,18]</sup>

The viologen moiety is attractive because its low-lying reduction potential provides a convenient electrochemical reporter group in supramolecular systems.<sup>[19–22]</sup> The low-energy LUMO allows for charge-transfer behaviour, which has been studied extensively, whereas the acidic *o*-bipyridinium hydrogen atoms also allow for charge-assisted hydrogen bonding.<sup>[23,24]</sup> The viologen group may, therefore, act as both a binding and a reporter group. We have reported previously, a 4,4'-bipyridine-derived hexasubstituted benzene receptor **5**, functionalised at only one end of the bipyridine.<sup>[24]</sup> This compound binds adenosine triphosphate (ATP), although all other anion binding is weak. In a preliminary communication, we also recently reported colourimetric anion sensing by a related tetrapodal, viologen-derived receptor.<sup>[25]</sup> We now report our full investigation into the synthesis, solution-state binding and spectroscopic prop-

[a] A. N. Swinburne, K. H. Fischer, S. J. Dickson, E. V. B. Wallace, Dr. A. Beeby, Prof. J. W. Steed  
Department of Chemistry, Durham University  
South Road, Durham, DH1 3LE (UK)  
Fax: (+44) 191-384-4737  
E-mail: jon.steed@dur.ac.uk

[b] M. J. Paterson  
Department of Chemistry, School of Engineering and Physical Sciences, Heriot-Watt University  
Edinburgh, EH14 4AS (UK)

[c] W. J. Belcher  
School of Mathematical and Physical Sciences  
University of Newcastle, Callaghan NSW 2308 (Australia)

Supporting information for this article is available on the WWW under <http://dx.doi.org/10.1002/chem.200902609>.

erties of a series of tri- and tetrapodal viologen-based anion receptors, based on the hexasubstituted benzene core.

## Results and Discussion

**Synthesis:** The synthesis of three tetrapodal viologen derivatives **2–4** was achieved by using the intermediate 1,1'-bis-(3,5-bis(bromomethyl)-2,4,6-triethylbenzyl-4,4'-bipyridine-1,1'-diium bromide (**1**), which can be synthesised in near quantitative yield through the reaction of excess 1,3,5-triethyl-2,4,6-tribromomethylbenzene with 4,4'-bipyridine (Scheme 1). Additional functionalisation can be achieved by treatment with pyridine, 1-pyridin-3-yl-3-*p*-tolyl-urea<sup>[26]</sup> and *N*-[(naphthalen-1-yl)methyl]pyridin-3-amine.<sup>[27]</sup> These reactions can be performed through traditional solution-state methods (compounds **2** and **6**) or alternatively by using a mechanochemical reaction (compounds **3** and **4**).<sup>[27]</sup> Yields vary from good to reasonable. The bromide salts of the tetrapodal receptors were metathesised to the hexafluorophosphate salt by precipitation of the product from a solution in methanol with  $\text{NH}_4\text{PF}_6$ .

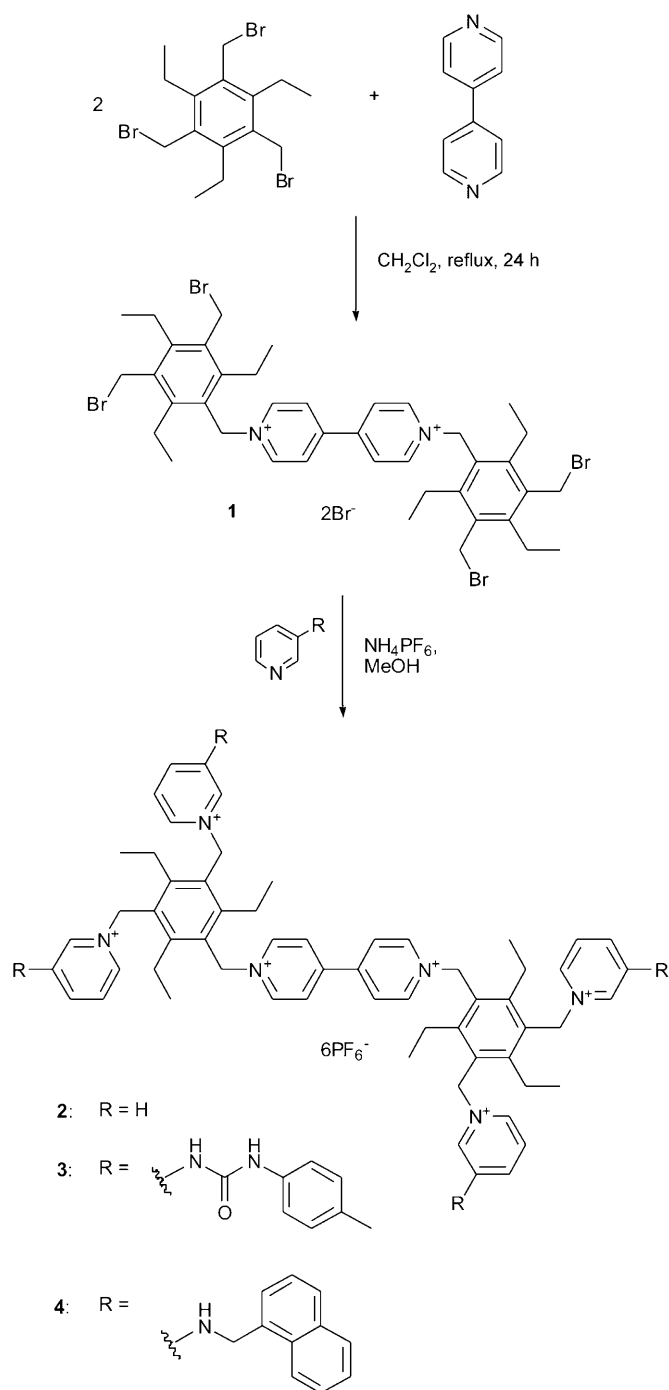
The tripodal tris(bipyridinium) receptor **6** is prepared in high yield from compound **5** by capping the three remaining bipyridyl nitrogen atoms with an excess of benzyl bromide in DMF at 50 °C. Again, anion metathesis to the hexafluorophosphate salt is achieved by the treatment of **6** with  $\text{NH}_4\text{PF}_6$ .

Several attempts were made to add various capping groups to compound **5**, such as methyl, ethyl, naphthyl and pyrenyl groups (Scheme 2). However, in all cases, except for **6**, no product or only partial capping resulted. The addition of capping groups was also attempted by using mechanochemical methods. Unfortunately, a mixture of 1, 2 and 3 capping groups was observed by using MALDI<sup>+</sup> mass spectrometry.

**Solution-state binding properties:** The anion binding properties of compounds **2–4** and **6** were investigated by using  $^1\text{H}$  NMR spectroscopy in  $\text{CD}_3\text{CN}$ . All of the compounds were shown to bind halides strongly. A 1:2 host/guest binding stoichiometry is suggested by  $^1\text{H}$  NMR spectroscopic titrations for compounds **2** and **3** and is supported by Job plot analysis. Figure 1 shows a representative Job plot for the tetrapodal receptor **2** with tetra-*n*-butylammonium (TBA) chloride.

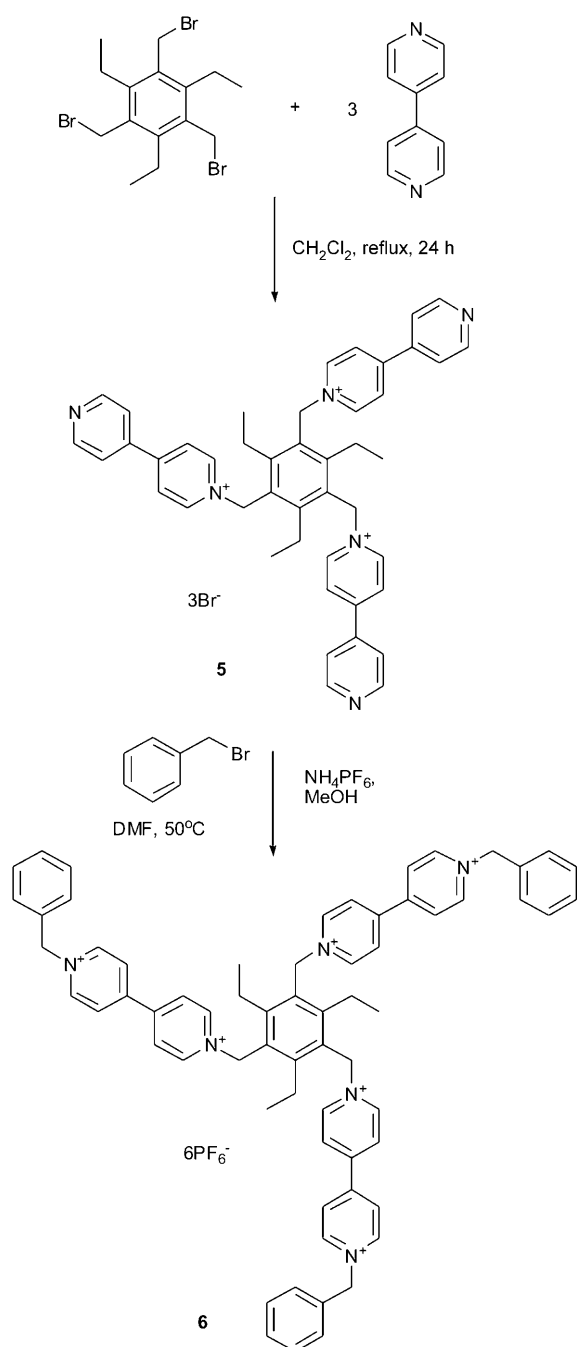
Compound **4** appears to have more complex speciation accompanied by a slow guest complexation or conformational change on the  $^1\text{H}$  NMR spectroscopic timescale as evidenced by significant broadening and splitting of several peaks at room temperature. As a result, binding constants could not be reliably determined.

The 1:2 binding stoichiometry observed in compounds **2** and **3** can be explained by the existence of two primary binding sites, which are essentially tripodal in nature. In the case of compound **2**, anion binding is due to hydrogen bonding from the *o*-pyridyl CH groups of the pyridinium and bi-



Scheme 1. Synthesis of tetrapodal anion receptors.

pyridinium units to the anion, as indicated by a downfield shift of the respective  $^1\text{H}$  NMR resonances. This  $\text{CH}\cdots\text{anion}$  interaction was shown to be important in previous systems.<sup>[8]</sup> An electrostatic contribution to binding is also likely. In the case of **3**, large downfield shifts are observed for the urea NH protons by  $^1\text{H}$  NMR spectroscopy, as well as smaller changes in the bipyridine and pyridinium resonances; indicative of hydrogen bonding.



Scheme 2. Synthesis of tripodal anion receptor **6**.

As with **2** and **3**, compound **6** exhibits a 1:2 host/guest binding stoichiometry. Downfield shifts were only observed for the  $^1\text{H}$  NMR resonances assigned to the *o*-pyridyl protons upon addition of anions, suggesting hydrogen bonding to those protons only. Again an electrostatic contribution to the binding is also likely.

It is difficult to imagine where a second halide anion could bind to compound **6**. One possibility is that the first anion sits low in the binding cavity near the hexasubstituted benzene ring, whereas the second sits high near the three benzyl groups. It could be imagined that hydrogen bonding

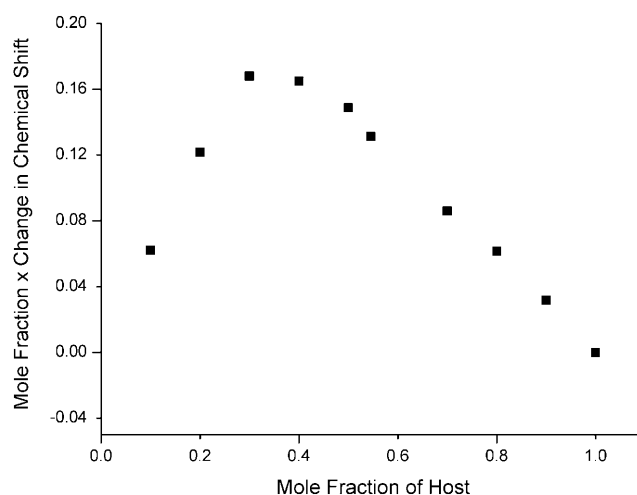


Figure 1. Job plot for compound **2** with TBA-Cl.

in this region would be weak because the distance between the binding arms is large. This is supported by  $^1\text{H}$  NMR spectroscopic evidence, since no significant chemical shift changes are seen for these “outer” protons. This model may also explain the low value of the second binding constant ( $K_{12} = \beta_{12} - \beta_{11}$ ) in the case of  $\text{Cl}^-$ . Even though chloride has the highest charge density, its small size means it may not be able to experience the full electrostatic attraction of all three arms. This would favour 1:2 binding for larger halides, as is observed. Table 1 contains the binding constants deter-

Table 1. Binding constants determined by  $^1\text{H}$  NMR spectroscopic titrations for compounds **2**, **3** and **6**.

Anion	Stoichiometry host/guest	<b>2</b>	<b>3</b>	<b>6</b>
$\text{Cl}^-$	1:1	4.30(6)	3.55(10)	3.98(13)
	1:2	7.83(5)	6.94(3)	4.855(2)
$\text{Br}^-$	1:1	3.66(6)	3.75(10)	3.63(4)
	1:2	6.93(5)	5.97(8)	6.03(12)
$\text{I}^-$	1:1	3.77(12)	3.58(13)	3.30(10)
	1:2	6.91(10)	6.55(7)	5.82(14)
$\text{NO}_3^-$	1:1	3.62(20)	2.89(3)	[a]
	1:2	6.64(3)	5.93(9)	[a]
$\text{HSO}_4^-$	[b]			
$\text{H}_2\text{PO}_3^-$	[b]			

[a] Data could not be refined. [b] Precipitated.

mined for compounds **2**, **3** and **6** by  $^1\text{H}$  NMR spectroscopic titration by using the least-squares curve-fitting program HypNMR 2006.<sup>[28]</sup>

In the case of compounds **2** and **6**, strong chloride binding is observed. Compound **3** exhibits interesting behaviour, in which bromide is bound strongly, with chloride and iodide bound more weakly. Nitrate is the weakest bound. Representative binding isotherms for the tetrapodal receptor **2** and tripodal receptor **6** are shown in Figures 2 and 3, respectively.

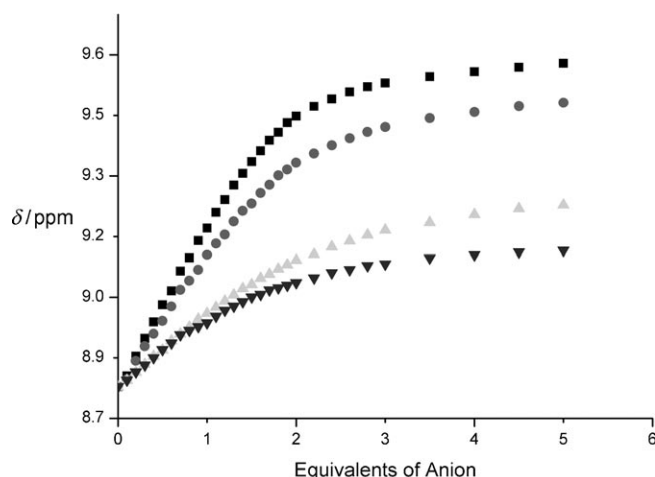


Figure 2. Binding isotherms for compound **2** with various anions: TBA-Cl (■), TBA-Br (●), TBA-I (▲), TBA-NO<sub>3</sub> (▼).

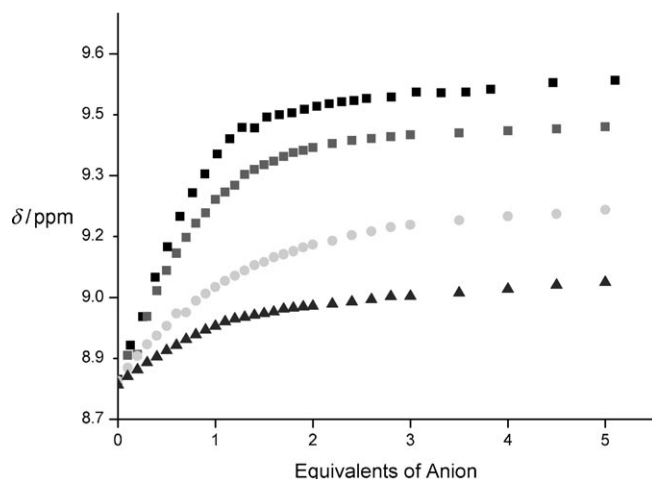


Figure 3. Binding isotherms for compound **6** with various anions: TBA-Cl (■), TBA-Br (●), TBA-I (▲), TBA-NO<sub>3</sub> (▼).

During <sup>1</sup>H NMR spectroscopic titration with carboxylate anions, a colour change from colourless to purple was observed. In aerated solutions this colour gradually fades to red and then orange upon standing, but the use of degassed solvent gave rise to a long-lasting purple colouration. <sup>1</sup>H NMR spectra in degassed solvent were recorded for compounds **2** and **6** in the presence of acetate. The purple colouration occurs immediately after the addition of acetate to compounds **2** and **6** and evidence of decomposition, in the form of new peaks in the <sup>1</sup>H NMR spectrum, is observed at two equivalents or above. This decomposition is likely to arise from the diffusion of oxygen into the tube during the experiment.

The <sup>1</sup>H NMR spectra for compound **2** upon addition of acetate shows large shifts are observed for the *o*-pyridyl ( $\Delta\delta = 0.36$  ppm) and *o*-bipyridyl ( $\Delta\delta = 0.3$  ppm) resonances consistent with the observations for halide binding (see the Supporting Information). In the case of **3**, large downfield shifts are observed for the resonances assigned to the urea

NH protons with only small shifts for the other resonances.<sup>[25]</sup>

The <sup>1</sup>H NMR spectra of **6** upon addition of acetate shows severe broadening of the resonances, with all peaks disappearing before one equivalent is reached. A <sup>1</sup>H NMR spectroscopic titration of compound **6** with TBA-malonate reveals downfield shifts in the bipyridyl resonances suggesting anion binding (see the Supporting Information).

Interestingly, in the case of **6**, a colour change is not observed with malonate until higher equivalents of guest are reached, even though NMR spectroscopic evidence suggests anion binding is occurring.

The cause of the decomposition of the carboxylate complexes of **2**, **3** and **6** is unknown. However, the viologen radical cation is known to be oxygen sensitive and the decomposition may be caused by hydroxide generated from dioxygen reduction by the radical cation. Evidence for the presence of the viologen radical cation has been found in the UV/Vis spectra of the charge-transfer complexes, as well as by Raman and ESR measurements (see below). The decomposition of the carboxylate complexes means that only qualitative information on carboxylate binding could be obtained by <sup>1</sup>H NMR spectroscopy.

An X-ray crystal structure determination of the hexafluorophosphate salt of compound **2** was undertaken. One independent hexacation is observed with PF<sub>6</sub><sup>−</sup> counterions, with a disordered acetonitrile pocket.

The compound adopts a *transoid* conformation with the triethylbenzene-derived units on opposite sides of the bipyridine. Each tripodal unit adopts a “two-up, one-down” conformation of the pyridinium groups. Although a “three-up” conformation is expected,<sup>[15–17]</sup> there is only a small energetic preference for this conformation, approximately 10 kJ mol<sup>−1</sup>, and the “two-up, one-down” conformation has been observed in similar systems.<sup>[8,9]</sup> The molecular structure (Figure 4) shows two of the PF<sub>6</sub><sup>−</sup> anions within the tripodal

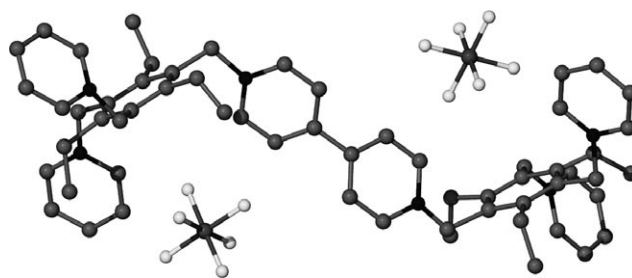


Figure 4. Molecular structure of compound **2** determined by X-ray crystallography. Hydrogen atoms removed for clarity.<sup>[25]</sup>

binding sites. This is consistent with the solution-state anion binding behaviour suggested by <sup>1</sup>H NMR spectroscopy. The anions are bound close to the viologen unit, which is a prerequisite for charge transfer.

**Variable-temperature <sup>1</sup>H NMR spectroscopic studies:** Variable-temperature <sup>1</sup>H NMR spectroscopic studies were under-

taken on compounds **2** and **6** in the presence and absence of chloride. Low-temperature  $^1\text{H}$  NMR spectroscopy in  $[\text{D}_6]\text{acetone}$  was used to help understand the conformations of the compounds. Figure 5 shows the  $^1\text{H}$  NMR spectrum of

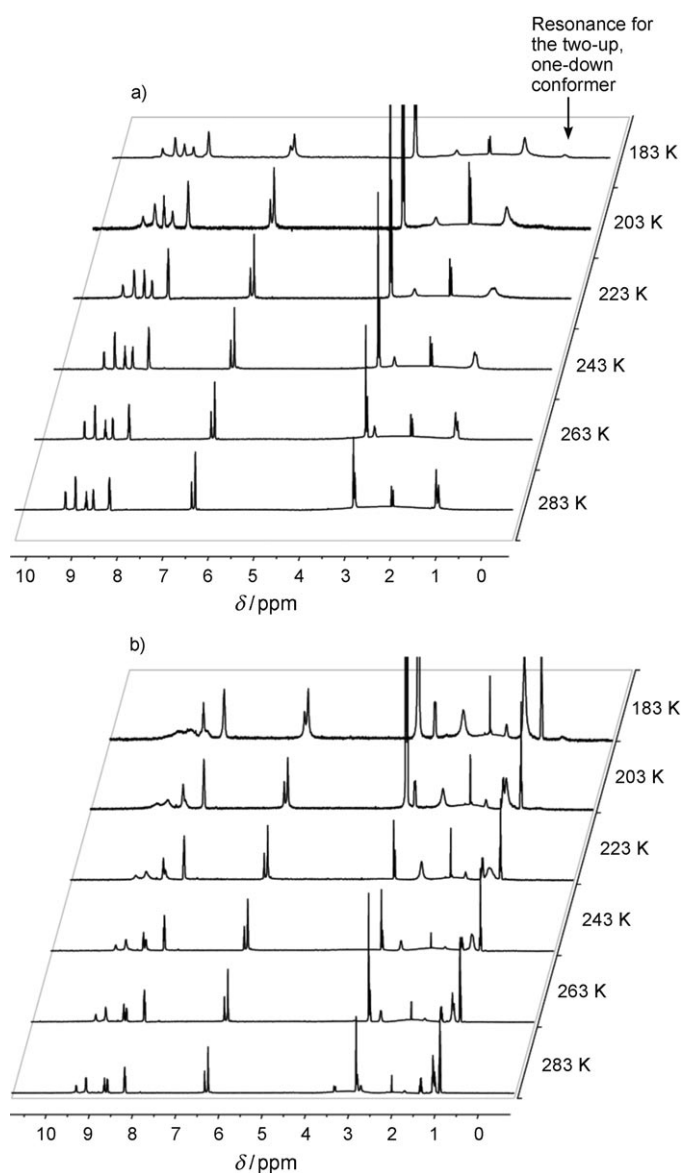


Figure 5. Variable-temperature  $^1\text{H}$  NMR spectra of a) compound **2** in  $[\text{D}_6]\text{acetone}$  and b) compound **2** in the presence of two equivalents of TBA-Cl. Solvent peaks have been removed for clarity (water at  $\delta = 2.13$  ppm and acetonitrile at  $\delta = 1.96$  ppm).

the hexafluorophosphate salt of host **2** as the temperature is lowered to 183 K. Broadening of the  $\text{CH}_2$  ( $\delta = 2.85$  ppm) and  $\text{CH}_3$  ( $\delta = 1.12$  ppm) resonances is observed. At 203 K the  $\text{CH}_3$  groups split from a single peak at 1.12 ppm to two peaks at  $\delta = 0.56$  and 1.29 ppm, corresponding to the “two-up, one-down” and “three-up” conformations, respectively. The upfield shift in the  $\text{CH}_3$  resonance is due to shielding of the methyl group by the pyridinium aromatic system when

the methyl substituent is on the same face as the pyridinium ring. There is also additional broadening and peak splitting in the aromatic region suggesting that a conformational exchange of the bipyridine protons is occurring.

The addition of two equivalents of TBA-Cl to **2** results in a downfield shift of the resonances assigned to the *o*-bipyridine protons causing overlap with another bipyridine peak (Figure 5). There is a marked reduction in the broadening of peaks at lower temperatures compared with the sample without added chloride. Significantly there is no sign of the two-up, one-down conformer observed in the free host, showing that the compound, in the presence of the  $\text{Cl}^-$  guest, adopts a threefold symmetrical (“three-up”) conformation at each tripodal unit. Interestingly, there is no evidence for an anion-exchange equilibrium, characterised by further splitting of the methyl and ethyl resonances, which has been observed in a related system.<sup>[8]</sup> At one equivalent of guest, the two-up, one-down conformer is still evident and shows that the two binding sites are not fully saturated.

The low-temperature  $^1\text{H}$  NMR spectra for compound **6** shows similar behaviour to that of **2** with broadening and eventual splitting of the  $\text{CH}_3$  (1.14 ppm) resonances into two peaks at  $\delta = 1.30$  and 0.42 ppm, corresponding to the three-up and two-up, one-down conformers, respectively (see the Supporting Information). The addition of chloride (1 equiv) still gives rise to a high-field  $\text{CH}_3$  resonance assigned to the two-up, one down conformer, although this is less intense and may be expected due to the 1:2 host/guest binding stoichiometry of the receptor. Further addition of chloride reduces the intensity of this resonance as both binding sites are populated, again suggesting a conformational change to a pseudo-threefold symmetric form upon anion binding.

**Charge-transfer behaviour:** Upon the addition of carboxylates, receptors **2**, **3**, **4** and **6** all give rise to an intense purple colouration with a band in the UV/Vis spectrum centred at approximately 540 nm (Figure 6). This absorption is assigned to an anion–viologen charge-transfer state. The particularly electron-deficient nature of the viologens in these compounds makes them excellent electron acceptors and charge-transfer behaviour in viologens is well known. Halides<sup>[29–31]</sup> (particularly iodide), electron-rich arenes,<sup>[32,33]</sup> phenols,<sup>[34,35]</sup> amines<sup>[36]</sup> and organic acids<sup>[34,37]</sup> all give rise to charge-transfer complexes with viologens.<sup>[23]</sup>

UV/Vis titrations were performed on compounds **2**, **3**, **4** and **6** with acetate, malonate and succinate (see Figures 7 and 8 for representative examples). Due to the air-sensitive nature of the complexes anaerobic conditions were necessary. Details of the procedure followed for the anaerobic UV/Vis titration can be found in the Supporting Information. A series of control experiments showed it was not possible to fully exclude oxygen from the experiment and a certain amount of decomposition occurs (discussed in the Supporting Information).

It has been reported that acetate forms a charge-transfer complex with methyl viologen (MV), with an intermolecular charge-transfer band at 405 nm and emission at 506 nm.<sup>[37]</sup>



Figure 6. a) Degassed  $1 \times 10^{-4}$  M solutions of host **2** in the presence of the TBA salts (1 equiv) of the following anions (from left to right): succinate, malonate, acetate, chloride, bromide, nitrate and perchlorate. b) Degassed  $1 \times 10^{-4}$  M solutions of hosts **6** in the presence of the TBA salts (1 equiv) of the following anions (from left to right): acetate, malonate, chloride, bromide, iodide and nitrate.

However, comparison of the band maxima of the methyl viologen diacetate complex (denoted  $MV \cdot (OAc)_2$ ) and the acetate complex of compound **2**, shows a large redshift of 135 nm. Similar shifts are observed for the other viologen-based receptors described herein. The  $MV \cdot (OAc)_2$  complex appears as a yellow/orange solution, whereas the tetrapodal viologen receptors, such as **2**, appear purple.

All of the compounds reach almost the exact same maximum absorbance value with acetate at a similar number of equivalents. Interestingly, upon addition of acetate to hosts **2**, **4** and **6**, an immediate colour change is observed. However, with host **3**, significant colouration does not appear until more than two equivalents of acetate are added. We interpret this result as implying binding-site competition between the different binding groups present. Compound **3** contains urea, as well as *o*-pyridyl, binding sites. At low equivalents, we propose that the acetate binds at the urea groups, away from the viologen unit; resulting in no charge transfer. As more equivalents are added and more  $PF_6^-$  ions are displaced, acetate is able to bind closer to the viologen and charge transfer is observed. This binding-site discrimination allows the tuning of the colourimetric response to the equivalents of guest added.

Malonate and succinate also cause a colourimetric response. Succinate causes significant colour changes for all compounds similar to acetate. Malonate, however, only causes significant colouration with compounds **2**, **3** and **4**. Compound **6** does not show significant colour change until higher equivalents are reached (approximately 20 equiv). A  $^1H$  NMR spectroscopic titration of compound **6** with TBA-malonate (see the Supporting Information) does suggest anion binding occurs and, therefore, it appears that the lack

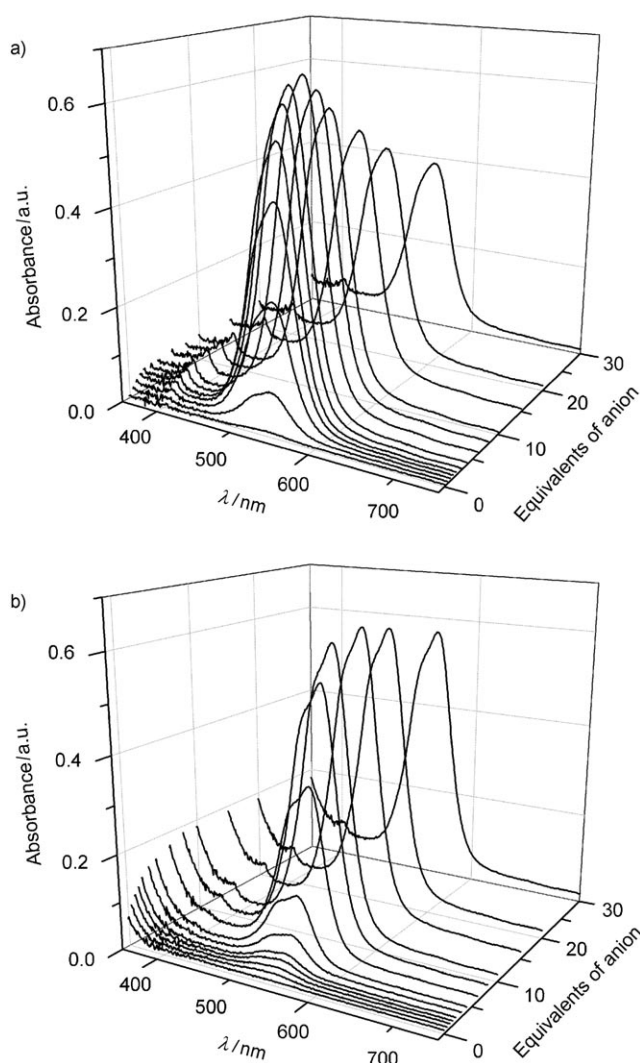


Figure 7. UV/Vis absorbance spectrum of a) compound **2** ( $1 \times 10^{-4}$  M in MeCN) and b) compound **3** ( $1 \times 10^{-4}$  M in MeCN) upon addition of TBA-acetate.

of charge transfer may be due to an unfavourable conformation of the complex, or is of electronic origin.

The UV/Vis spectroscopic titration of compound **6** with TBA-acetate results in a broadened band at 540 nm and a very prominent band at 396 nm (Figure 8). In contrast, in the tetrapodal receptors **2–4** this band is significantly lower in intensity. The band at 396 nm is consistent with the absorbance profile of the viologen radical cation (bands at 396 and 608 nm)<sup>[23,38]</sup> and the broadening of the 540 nm band is likely to be due to overlap with the 608 nm band of the radical cation. The band is also observed to a lesser extent for compound **2** and suggests that in addition to the formation of a charge-transfer complex, an electron-transfer process is also occurring, particularly in **6** (see below).

**DFT calculations:** DFT calculations were undertaken to test the feasibility of the proposed binding model and to inter-



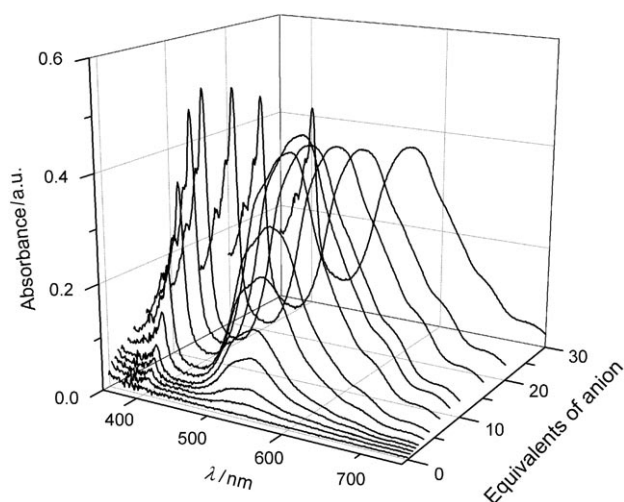


Figure 8. UV/Vis absorbance spectrum of compound **6** ( $1 \times 10^{-4}$  M in MeCN) upon addition of TBA-acetate.

pret the  $^1\text{H}$  NMR and UV/Vis spectroscopic data. Structures were optimised by using B3LYP/4-31G on the host, with the hydrogen atoms proximal to the anion augmented with additional s and p diffuse functions and the 6-31+G\* basis set on the anion. Electronic transitions were calculated by using time-dependent (TD)-DFT with the B3LYP functional and the 6-31G\* basis set on all atoms.

The optimised structure of the receptor, **2**, with acetate (Figure 9) reveals a *transoid* conformation with the acetate

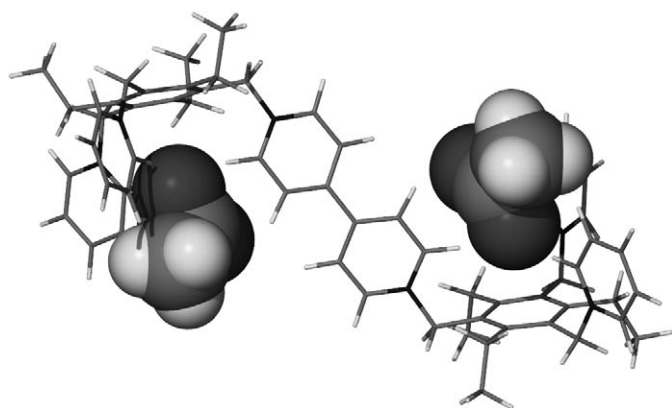


Figure 9. Optimised geometry for compound **2** with acetate.

bound by pyridinium  $\text{CH}\cdots\text{O}$  hydrogen-bonding interactions. Crucially, the structure suggests that the acetate is held in close proximity to the viologen core, which would facilitate a charge-transfer process.

The calculated structure of **3** with acetate demonstrates binding of the acetate to the urea functional groups (Figure 10), consistent with  $^1\text{H}$  NMR spectroscopic titrations, and are remote from the viologen. TD-DFT calculations do not show a corresponding charge-transfer band at

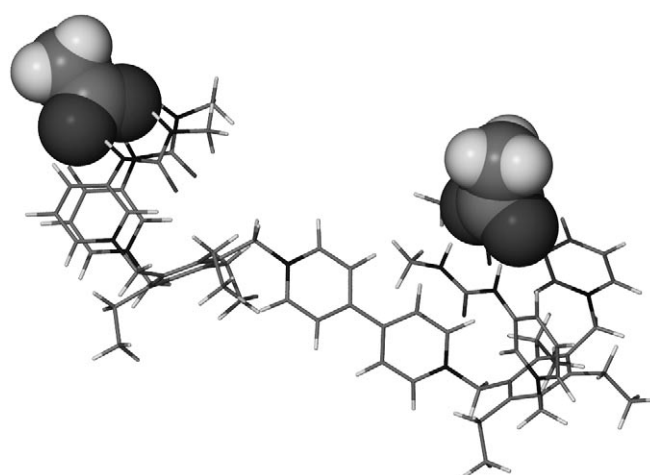


Figure 10. Optimised geometry for the **3** with two equivalents of acetate.

550 nm. This is consistent with the delayed evolution of the purple colouration of the complex.

The optimised structure of **2** with malonate is shown in Figure 11. The flexible nature of the receptor allows the

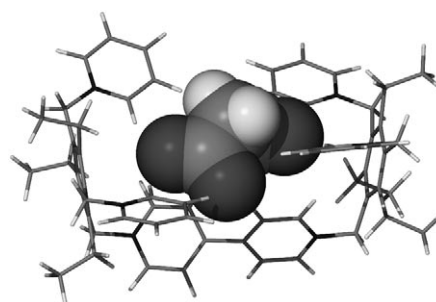


Figure 11. Optimised geometry for compound **2** with malonate.

compound to encapsulate the malonate in a *cisoid* manner. The malonate is bound by charge-assisted pyridinium  $\text{CH}\cdots\text{O}$  interactions. The anion is situated close to the viologen in a suitable geometry to allow a charge-transfer interaction. TD-DFT calculations suggest a transition involving the promotion of an electron in a localised  $\pi$  orbital on the malonate anion to the  $\pi^*$  orbital on the bipyridinium moiety (Figure 12). The transition has a large oscillator strength ( $f=0.005$ ) and so would be expected to give rise to an intense vibronic band, consistent with observation.

The optimised structure of **6** with acetate, Figure 13, suggests a three-up conformation in which the anion is bound by three charge-assisted hydrogen bonds, one of the acetate oxygen atoms is bound by two hydrogen bonds, whereas the second is bound by only one. Again, TD-DFT calculations show a  $\pi \leftarrow \sigma$  transition at 560 nm with an oscillator strength of 0.004 (Figure 14), comparable to **2** with malonate.

All of the charge-transfer complexes described above show unusually low-energy charge-transfer bands compared with the typical complexes of methyl viologen suggesting

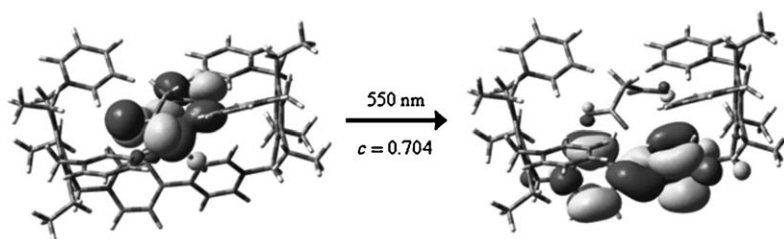


Figure 12. Calculated electronic transition of **2** with malonate showing charge transfer from the anion to the viologen moiety.

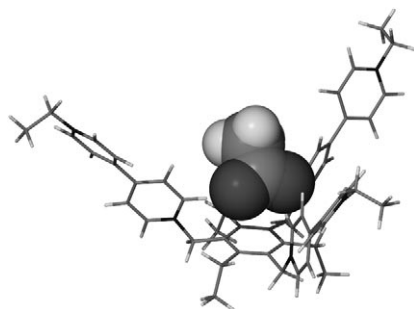


Figure 13. Optimised geometry for **6** with acetate.

that these polycationic hosts are particularly readily reduced. To try and understand this observation, an electrochemical investigation of the hosts was undertaken.

**Electrochemistry:** The electrochemistry of viologen derivatives has been extensively investigated.<sup>[39]</sup> They exhibit two reversible redox couples, the first of which, formation of the radical cation from the dication, is the most reversible and has an unusually low reduction potential for an organic molecule.

As a control, the reduction potential of methyl viologen dihexafluorophosphate, (denoted MV•(PF<sub>6</sub>)<sub>2</sub>) was measured in 0.1 M TBA-PF<sub>6</sub> in MeCN by using a Pt working electrode. The reduction potentials were found to be  $E_1 = -0.42$  and  $E_2 = -0.83$  versus SCE and are consistent with literature values measured under similar conditions.<sup>[38,39]</sup> The peak to peak separation is close to the value expected for a single-electron process and shows no significant variation with

Table 2. Summary of electrochemical data for viologen derivatives,  $E_{1/2}$  values reported versus SCE.

Compound	$E_{1/2}$ [V]	$\Delta E$ [mV]	$I_{pa}/I_{pc}$
<b>2</b>	-0.36	70	0.9
	-0.74	70	> 0.9
<b>3</b>	-0.31	110	> 0.9
	-0.76	90	0.7
<b>4</b>	-0.35	100	0.9
	-0.74	60	> 0.9
<b>6</b>	-0.34	60	> 0.9
	-0.76	70	> 0.9

rapodal derivatives the peak to peak separation is generally higher than for MV•(PF<sub>6</sub>)<sub>2</sub>.

This overpotential may be due to an unfavourable conformational change required for the viologen to approach the electrode or upon accepting the electron. It is also observed that the anode/cathode peak ratio is not as high as with MV, although good reversibility is still found in most cases. The cyclic voltammogram of compound **2** at a scan rate of 100 mV s<sup>-1</sup> is shown as a representative example (Figure 15).

Compound **6** shows behaviour almost identical to that of MV<sup>2+</sup>, with good reversibility, except with slight broadening of the radical cation reduction peak (Figure 16).

In all cases, a significantly more cathodic first and second redox potential is found when compared with MV<sup>2+</sup>, with a cathodic shift of at least 70 mV. A possible explanation may lie with the electron-withdrawing effect of the viologen substituents. For example, for the tetrapodal derivatives the two quaternised pyridinium nitrogen atoms give each substituent a formal two-plus charge. It has been shown that the reduc-

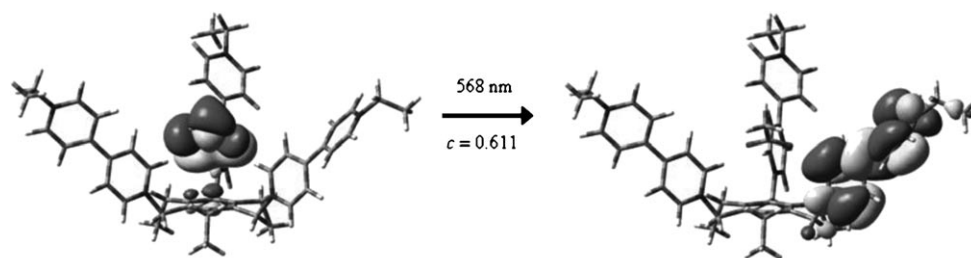


Figure 14. Major component of the calculated electronic absorbance of **6** with acetate showing charge transfer from the anion to the viologen moiety.



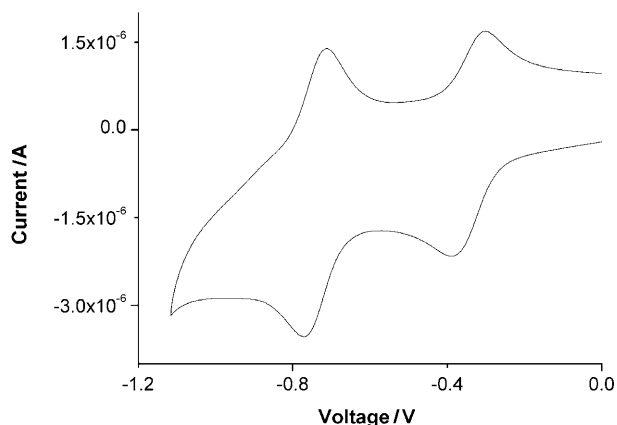


Figure 15. Cyclic voltammogram of compound **2** at a  $100 \text{ mVs}^{-1}$  scan rate.

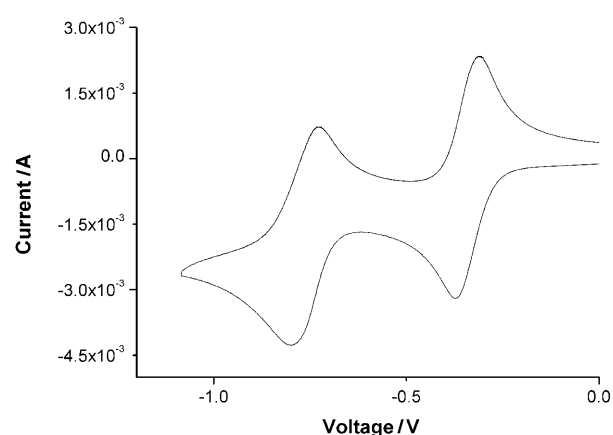


Figure 16. Cyclic voltammogram of compound **6** at a  $100 \text{ mVs}^{-1}$  scan rate.

tion potential of viologens obeys a linear free-energy relationship (LFER) with the nitrogen substituents and that electron withdrawing groups increase the reduction potential.<sup>[23,39,40]</sup>

**Electrochemical titrations:** It has been shown that the anion can play a significant role in determining the reduction potential of viologens. In many cases, only a small potential shift is found, but this is not always the case.<sup>[39]</sup> The effect on the redox potential of the addition of anion to compounds **2**, **3**, **4** and **6** was investigated. Since these receptors are able to bind halides strongly, close to the viologen unit, it was anticipated that significant perturbation of the redox wave would be observed. Ferrocene ( $\text{Fc}/\text{Fc}^+$ ) was used as an internal reference. Control titrations with anions and an aqueous  $\text{Ag}/\text{AgCl}$  electrode proved that no significant change in the ferrocene redox wave was observed with added anion. A scan rate of  $200 \text{ mVs}^{-1}$  was used with the electrochemical cell kept under a constant positive pressure of  $\text{N}_2$ . The guest solutions were degassed before use (see the Experimental Section).

Almost identical behaviour was seen for compounds **2**, **3** and **4** upon the addition of TBA-Cl. As the number of equivalents is increased, a gradual increase in peak intensity is observed with a low to modest anodic potential shifts (e.g., compound **2**,  $\Delta E = 80 \text{ mV}$  with TBA-Cl (30 equiv)). Both the potential shift and current increase were consistent for compounds **2**, **3** and **4**. A representative stack plot is shown in Figure 17. Significantly, smaller intensity gains and

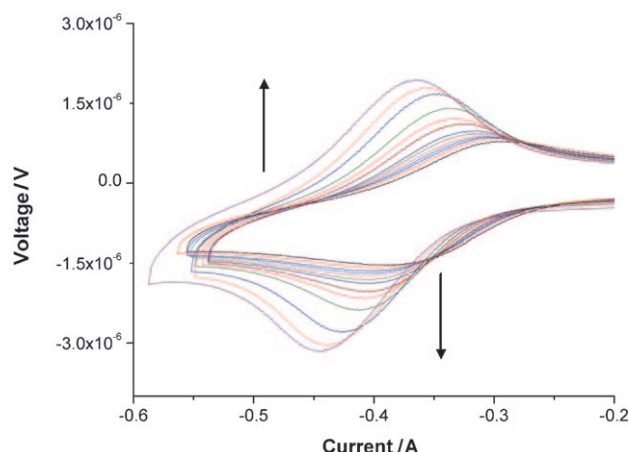


Figure 17. Cyclic voltammogram of compound **2** ( $1 \times 10^{-4} \text{ mol dm}^{-3}$ ) with increasing equivalents (0, 0.5, 1, 1.5, 2, 3, 4, 6, 8, 10, 15, 20 and 20 equiv) of TBA-Cl.

potential shift was observed for TBA-Br ( $\Delta E = 14 \text{ mV}$ ). These titrations do show that addition of anions does affect the cyclic voltammograms obtained and hence, the viologen redox potential.

Compound **6** demonstrates a unique property in this series of compounds. At 25 equivalents of TBA-Cl a shoulder appears at lower potential on the anodic peak. With the addition of further chloride, this shoulder grows and the original peak is reduced (Figure 18). The cathodic peak is also reduced. This same effect is also observed to a lesser

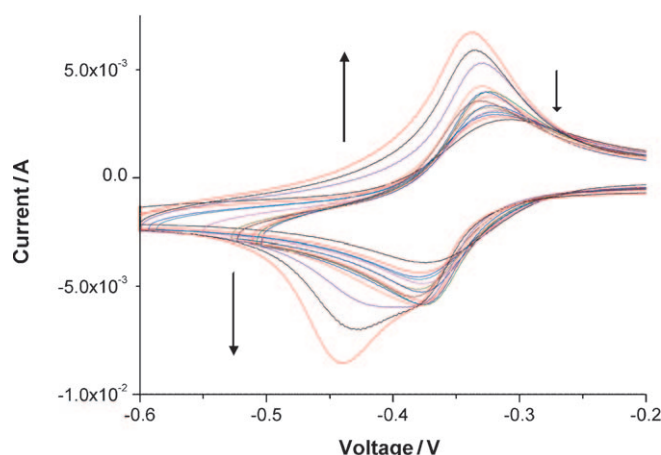


Figure 18. Cyclic voltammogram of compound **6** ( $1 \times 10^{-4} \text{ mol dm}^{-3}$ ) with increasing equivalents (0, 0.5, 1, 1.5, 2, 3, 4, 6, 8, 10, 15, 20 and 20 equiv) of TBA-Cl.

extent for TBA-Br. Addition of TBA-Cl (30 equiv) and repeated scanning, without further addition of anion, also leads to the growth of the shoulder. Thorough cleaning of the electrode surface produced a scan similar to the original scan. This suggests that deposition of the complex on the electrode surface occurs at higher equivalents of halide guest. A similar effect has recently been reported by Gale and co-workers<sup>[41]</sup> with ferrocene-derived phenylenediamine anion receptors. They suggest the effect of electrodeposition may provide a new means of anion sensing.

Titration with acetate, malonate and succinate anions were also undertaken for all of the compounds. There is general trend for a gradual decrease in peak intensity as more anion is added in all cases. This is accompanied by a colour change from colourless to purple. In the case of **3**, colour change does not occur until after the addition of several equivalents of anion; there is an increase in the peak current before eventually the current decreases substantially. A possible interpretation of this data would be that the formation of the anion–viologen charge-transfer complex results in a significant rise in the energy of the viologen LUMO, making the electron transfer from the electrode more unfavourable. The decrease in the current intensity should then be proportional to the ratio of bound/unbound host with only the unbound host, giving an electrochemical response. At higher equivalents of anion, when the amount of unbound host is low, the current intensity is low.

Given the low reduction potential of the host molecules described above, in principle it should be relatively easy to chemically reduce the viologen unit to the radical cation. Indeed, there is evidence for this in the UV/Vis spectra of the charge-transfer complexes, particularly for compounds **2** and **6** with acetate, which show a significant band at 398 nm and the appearance of a tail on the charge-transfer band. These bands are assigned to the formation of a viologen radical cation.

**Investigation into the radical cation:** The spectroscopy of the viologen radical cation has been extensively studied.<sup>[23]</sup> The UV/Vis spectra of the chemically reduced MV·PF<sub>6</sub>, MV·OAc and compound **2** are shown in Figure 19. The MV·OAc radical cation is formed upon the addition of TBA·OAc to methyl viologen dihexafluorophosphate. It appears that the reaction of MV<sup>2+</sup> and acetate ions in a relatively noncompetitive solvent, leads to ion pairing and electron transfer, with no evidence of a charge-transfer band in the UV/Vis spectrum.<sup>[37]</sup> Generation of the radical cation from charge-transfer complexes is known and generally occurs by a photoelectron-transfer process.<sup>[23,42]</sup> However, typically, back-electron transfer is fast and transient absorption spectroscopy is required to observe the radical.<sup>[42]</sup> All of the spectra shown in Figure 19 are essentially identical, suggesting that the R groups on compound **2** and the change in counterion have no effect on the optical transitions of the radical and are consistent with the literature values.<sup>[23,38]</sup>

To confirm the presence of the cation radical, ESR spectroscopy studies on compounds **2** and **6** were undertaken in

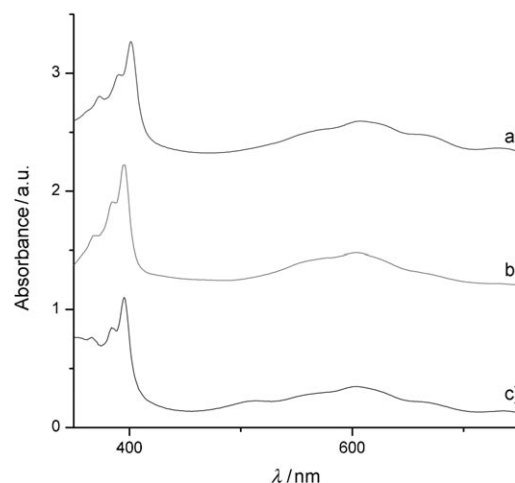


Figure 19. UV/Vis spectra of the radical cation of viologen derivatives. a) Compound **2**; b) MV·OAc; c) MV·PF<sub>6</sub>.

acetonitrile at 205 K. Compound **6** does show a weak resonance (Figure 20) with a *g* factor of 2.0065, close to the value of a free electron and close to the literature value for MV.<sup>[43]</sup> The resonance does not show any hyperfine struc-

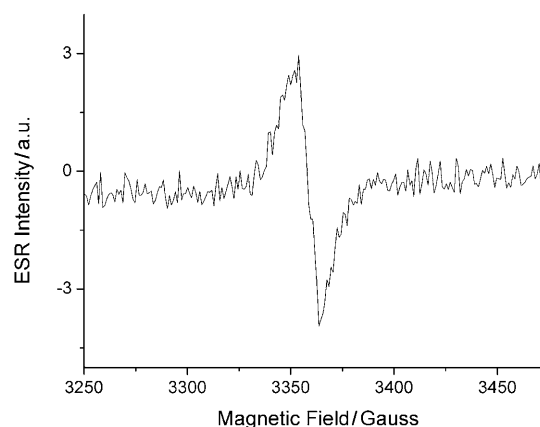


Figure 20. ESR spectrum for compound **2** in acetonitrile at 205 K.

ture. No ESR spectroscopic resonance was observed for compound **2**, however, this is not unexpected. When comparing the UV/Vis spectra of the acetate complexes of **2** and **6**, there is significantly less intensity of the 398 nm band for compound **2**. Given the weak signal obtained for **6** (attenuated by the strongly microwave absorbing solvent, acetonitrile), a very weak signal would be expected for **2**.

The viologen radical cation can also be probed by using resonance Raman spectroscopy.<sup>[44–47]</sup> Figure 21 shows the resonance Raman spectrum of the MV·PF<sub>6</sub> radical cation, measured with a 633 nm He–Ne laser. The peaks correspond to those reported in the literature.<sup>[44]</sup> A resonance Raman spectrum was also obtained for the charge-transfer complex of **2** with acetate, targeting the charge-transfer band by using a Nd:YAG laser at 532 nm (Figure 21). Several peaks

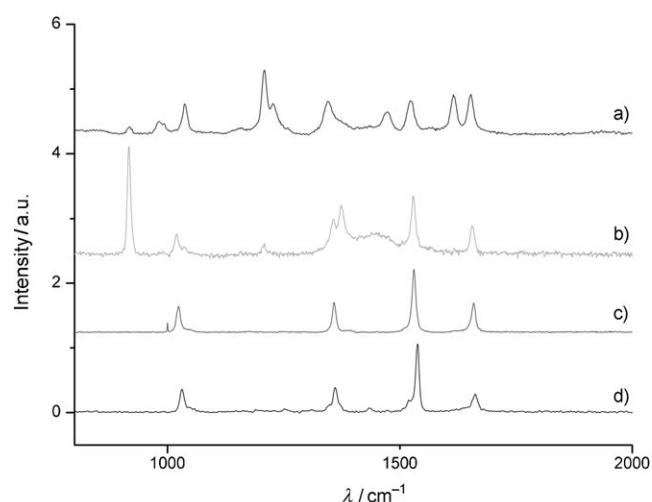


Figure 21. Resonance Raman spectra for viologen derivatives: a) **2** with acetate (532 nm), b) **2** with acetate (633 nm), c) chemically reduced **2** radical and d) MV·PF<sub>6</sub> radical.

appear in the spectral region corresponding to bipyridine vibrations, four of which broadly correspond to the radical bands. A resonance Raman spectrum was also obtained for the same complex by using the He–Ne laser at 633 nm (Figure 21). The absorbance of the charge-transfer band is essentially zero at this wavelength, whereas the absorbance of the radical cation is relatively high. Correspondingly, four prominent bands appear in the spectrum, which correspond well to the radical cation. Therefore, depending on the wavelength used, both the charge-transfer complex and the radical cation or radical cation alone can be targeted.

Interestingly, compound **6** has identical resonance Raman spectra for the charge-transfer complex and the radical cation as compound **2**. Given the symmetry differences in the compounds, this suggests that the orbitals involved in the radical cation electronic transition are localised almost entirely on the bipyridine unit. The band at 950 cm<sup>-1</sup> is present in all spectra containing an acetate anion and is tentatively assigned as an acetate vibration.

## Conclusion

Four viologen-derived anion hosts have been synthesised with either a ditopic, tetrapodal or a monotopic, tripodal design. All of the compounds bind anions strongly in acetonitrile, with a colourimetric response observed only upon the addition of carboxylates. Carboxylates give rise to an absorbance band centred at 540 nm. This is assigned to a charge-transfer interaction, an assignment supported by DFT calculations. The band is redshifted significantly compared with related systems in the literature<sup>[23]</sup> and is due to the very low reduction potential of the viologen derivatives synthesised in this work.

Cyclic voltammetric titrations have shown that there are modest anodic shifts in the reduction potential, but signifi-

cant increases in the peak current. For compound **6**, titrations with chloride gave rise to an anodically shifted electro-deposition peak. Titrations with acetate caused the loss of the viologen redox wave, the cause of which is preliminarily assigned to the high energy of the viologen LUMO as a result of the charge-transfer interaction preventing the typical viologen reduction occurring.

Addition of carboxylates also gives rise to the radical cationic species of the viologen derivatives, particularly for compounds **2** and **6**. The radical cation was characterised by UV/Vis, Raman and ESR spectroscopies.

By coupling tripodal anion binding groups to a viologen-type reporter it is possible to develop and tune a colourimetric sensor for carboxylate anions. The anion response can be modulated by the presence of other anion binding groups that control access to the chromophore and, in the case of **6** and malonate, these appear to depend on the anion binding geometry.

## Experimental Section

**Instrumentation:** All NMR spectroscopy was performed on a Varian Mercury-400 (400 MHz for <sup>1</sup>H), Varian Inova-500 machine (500 MHz for <sup>1</sup>H, 126 Hz for <sup>13</sup>C) or a Varian DD-700 (700 MHz for <sup>1</sup>H, 176 MHz for <sup>13</sup>C) spectrometer and were referenced to residual solvent. Electrospray (ES) mass spectroscopy was recorded on a Thermo-Finnigan LTQ instrument, whereas MALDI experiments were recorded on an ABI Voyager-DC STR instrument. Elemental analysis was performed by using an Exeter Analytical CE-400 Elemental Analyser. All Raman spectra were obtained on a Horiba Jobin–Yvon LabRAM HR instrument equipped with an Nd:YAG (532 nm), He–Ne (633 nm) laser. Spectra were acquired by using a 600 g/mm diffraction grating and an Andor CCD detector. Band positions were calibrated against silicon. The software used was Labspec 5. FTIR were recorded with a Perkin–Elmer Spectrum 100 ATR instrument (Perkin–Elmer, Norwalk, CT, USA). For each spectrum, 64 scans were conducted over a spectral range of 4000 to 600 cm<sup>-1</sup> with a resolution of 4 cm<sup>-1</sup> (def=deformation). The analysis was carried out with the Spectrum Express 1.01 software. ESR spectra were recorded on a Bruker BioSpin EMX spectrometer at 205 K. All solid-state reactions were carried out by using a Retsch MM200 ball mill with a 25 mL shaker grinding jar.

**General procedure for <sup>1</sup>H NMR spectroscopy titrations:** <sup>1</sup>H NMR titration experiments were carried out at room temperature by using a Varian Inova-500 (500 MHz for <sup>1</sup>H) or a Varian Mercury-400 (400 MHz for <sup>1</sup>H) spectrometer (Durham University). All chemical shifts are reported in ppm relative to residual solvent. A solution of the host species of known concentration, typically 0.5–1.5 mM, was made up in an NMR tube in the appropriate deuterated solvent (0.5 mL). Solutions of the anions, as TBA salts (1 mL), were made ten times the concentration of the host solution. The guest solution was typically added in aliquots (10 μL), representing 0.1 equiv of the guest with respect to the host. Larger aliquots were used in some cases in which no inflection of the trace was evident. Spectra were recorded after each addition and the trace was followed simultaneously. Results were analysed by using the curve-fitting program HypNMR 2006.<sup>[28]</sup>

**General procedure for UV/Vis spectroscopic titrations:** UV/Vis titrations were carried out by using an ATI–Uinacam UV2 UV/Vis spectrometer. A solution of host (1 × 10<sup>-4</sup> mol dm<sup>-3</sup>) was made in a volumetric flask. A 3 mL sample of host solution (1 × 10<sup>-5</sup> mol dm<sup>-3</sup>) was prepared by dilution of the stock solution. Guest solutions were prepared such that 300 μL of guest solution corresponded to 10 equivalents of host. Solutions were prepared by using dry degassed acetonitrile as solvent. All samples were prepared in a glove box and were sealed with Suba-Seals and Parafilm.

A nitrogen balloon was used to maintain an inert atmosphere during removal or addition of aliquots of solution.

**General procedure for cyclic voltammetry experiments:** Cyclic voltammetry was carried out on a Chi Instruments Model 420 Electrochemical Analyser by using two Pt wire counter electrodes and a 2 mm Pt working electrode or a 3 mm glassy carbon working electrode. The ferrocene/ferrocenium redox couple was used as an internal reference.  $E_{1/2}$  values are reported versus SCE ( $Fc=0.40$  V with TBA- $PF_6$  in MeCN<sup>[48]</sup>). A solution of TBA- $PF_6$  (0.1 mol dm<sup>-3</sup>) in dry MeCN was used as the electrolyte. Solutions were degassed by bubbling through N<sub>2</sub> and the cell was kept under a positive pressure of N<sub>2</sub> at all times.

**General procedure for cyclic voltammetry titration experiments:** A host solution (1 × 10<sup>-4</sup> mol dm<sup>-3</sup>) with TBA- $PF_6$  in MeCN (0.1 mol dm<sup>-3</sup>) was used. Guest solutions were prepared such that 300 µL of guest solution corresponded to 10 equivalents of host and were degassed by bubbling through N<sub>2</sub>. A scan rate of 200 mV s<sup>-1</sup> was used for all scans.

Materials were obtained from standard commercial sources. 1,3,5-Tri(bromomethyl)-2,4,6-triethylbenzene was prepared as previously reported.<sup>[49]</sup>

**Synthesis of 1:** 1,3,5-Tri(bromomethyl)-2,4,6-triethylbenzene (6.00 g, 13.60 mmol) and 4,4'-bipyridine (0.21 g, 1.36 mmol) were dissolved in dichloromethane (150 mL) and stirred at reflux for 20 h. During this time, a pale yellow precipitate of 1,1'-bis(3,5-bis(bromomethyl)-2,4,6-triethylbenzyl)-4,4'-bipyridine-1,1'-dium bromide was formed. This was filtered and washed with dichloromethane (3 × 50 mL). This yielded the bromide salt as a pale yellow solid (1.32 g, 1.27 mmol, 93 %). M.p. 250 °C dec; <sup>1</sup>H NMR ([D<sub>6</sub>]DMSO, 500 MHz): δ = 9.01 (d, *J* = 7.0 Hz, 4H; *Hobipy*), 8.71 (d, *J* = 7.0 Hz, 4H; *Hmbipy*), 6.05 (s, 4H; -CH<sub>2</sub>-Py<sup>+</sup>), 4.78 (s, 8H; -CH<sub>2</sub>Br), 2.96 (q, *J* = 7.3 Hz, 4H; -CH<sub>2</sub>CH<sub>3</sub>), 2.76 (q, *J* = 7.3 Hz, 8H; -CH<sub>2</sub>CH<sub>3</sub>), 1.34 (t, *J* = 7.3 Hz, 6H; -CH<sub>2</sub>CH<sub>3</sub>), 1.07 ppm (t, *J* = 7.3 Hz, 12H; -CH<sub>2</sub>CH<sub>3</sub>); <sup>13</sup>C{<sup>1</sup>H} NMR ([D<sub>6</sub>]DMSO, 100 MHz): δ = 149.8, 147.6, 147.1, 145.3, 134.3, 127.8, 127.2, 58.3, 31.4, 23.6, 23.2, 16.0 ppm; IR: ν̄ = 3120 (s, Ar C-H), 3044 (s, Ar C-H), 2967 (s, CH<sub>2</sub>/CH<sub>3</sub>), 2923 (s, CH<sub>2</sub>/CH<sub>3</sub>), 2879 (s, CH<sub>2</sub>/CH<sub>3</sub>), 1636 (s, Ar C=C), 1560 (s, Ar C=C), 1501 (m, Ar C=C), 1444 (s, CH<sub>2</sub>/CH<sub>3</sub> def), 1381 (m, CH<sub>3</sub> def), 699 (m, C-Br), 587 (m, C-Br), 509 cm<sup>-1</sup> (m, C-Br); MS (ES<sup>+</sup>): *m/z* (%): 878 [M-2Br]<sup>+</sup> (2 × <sup>81</sup>Br + 2 × <sup>79</sup>Br), 517 [M]<sup>2+</sup> (1 × <sup>81</sup>Br + 5 × <sup>79</sup>Br), 494, 439 [C<sub>20</sub>H<sub>23</sub>Br<sub>2</sub>N]<sup>+</sup> (1 × <sup>81</sup>Br + 1 × <sup>79</sup>Br), 361 [C<sub>15</sub>H<sub>19</sub>Br]<sup>+</sup> (2 × <sup>81</sup>Br), 349, 305, 261 [M]<sup>4+</sup> (6 × <sup>81</sup>Br), 217, 179 [M-4Br]<sup>4+</sup> (2 × <sup>79</sup>Br); elemental analysis calcd (%) for C<sub>40</sub>H<sub>50</sub>N<sub>2</sub>Br<sub>6</sub>: C 44.72, H 4.85, N 2.70; found: C 44.43, H 4.80, N 2.51.

**Synthesis of 2:** Compound 1 (0.25 g, 0.24 mmol) and pyridine (2.85 g, 36 mmol) were dissolved in methanol (125 mL) and stirred at reflux for 6 h. The reaction mixture was then cooled and the solvent (105 mL) removed under reduced pressure. Diethyl ether (30 mL) was added to the solution and a yellow precipitate was observed. This was filtered and a <sup>1</sup>H NMR spectrum was taken of the bromide salt. The resultant precipitate was sticky and was not fully characterised. The solid was dissolved in methanol (30 mL) with NH<sub>4</sub>PF<sub>6</sub> (10 equiv, 0.39 g, 2.41 mmol) and stirred at ambient temperature for 6 h. A very pale yellow precipitate of 1,1'-bis(2,4,6-triethyl-3,5-bis(pyridinium-1-ylmethyl)benzyl)-4,4'-bipyridine-1,1'-dium hexafluorophosphate was observed, which was recovered by filtration and dried under ambient conditions. The solid was recrystallised from acetonitrile and diethyl ether, producing a sticky, pale yellow solid. This was filtered, redissolved in acetonitrile (10 mL) and then the solvent was removed under reduced pressure to give a pale yellow solid powder (0.23 g, 0.13 mmol, 55 %). M.p. 230 °C dec; <sup>1</sup>H NMR ([D<sub>6</sub>]DMSO, 500 MHz): δ = 9.17 (d, *J* = 6.7 Hz, 4H; *Hobipy*), 8.93 (d, *J* = 6.2, 8H; PyH), 8.65 (m, 8H; *Hmbipy* and PyH), 8.18 (t, *J* = 7.1 Hz, 8H; PyH), 6.14 (s, 4H; -CH<sub>2</sub>Py), 6.08 (s, 8H; -CH<sub>2</sub>Py), 2.69 (q, *J* = 7.5 Hz, 12H; -CH<sub>2</sub>CH<sub>3</sub>), 0.82 ppm (m, 18H; -CH<sub>2</sub>CH<sub>3</sub>); <sup>13</sup>C{<sup>1</sup>H} NMR ([D<sub>6</sub>]DMSO, 100 MHz): δ = 151.1, 151.0, 150.0, 146.9, 145.7, 144.7, 129.2, 129.0, 128.4, 127.6, 58.4, 58.1, 24.2, 15.5, 15.4 ppm; IR: ν̄ = 3143 (m, Ar C-H), 3104 (m, Ar C-H), 2978 (m, CH<sub>2</sub>/CH<sub>3</sub>), 2940 (m, CH<sub>2</sub>/CH<sub>3</sub>), 1637 (s, Ar C=C), 1567 (s, Ar C=C), 1503 (s, Ar C=C), 1485, 1448 (m, CH<sub>2</sub>/CH<sub>3</sub> def), 1391 (m, CH<sub>3</sub> def), 1219, 1149, 1043, 838, 558 cm<sup>-1</sup>; MS (ES<sup>+</sup>): *m/z*: 805 [C<sub>35</sub>H<sub>39</sub>N<sub>3</sub>P<sub>6</sub>F<sub>12</sub>]<sup>+</sup>, 728 [M-2(PF<sub>6</sub>)]<sup>2+</sup>, 519, 437 [M-6(PF<sub>6</sub>)]<sup>2+</sup>, 437 [M-3(PF<sub>6</sub>)]<sup>3+</sup>, 330, 291 [M-4(PF<sub>6</sub>)]<sup>4+</sup>, 275, 259, 227, 212, 204 [M-5(PF<sub>6</sub>)]<sup>5+</sup>; elemental analysis calcd (%) for C<sub>60</sub>H<sub>70</sub>N<sub>6</sub>P<sub>6</sub>F<sub>36</sub>: C 41.30, H 4.04, N 4.82;

found: C 41.77, H 4.14, N 4.75. Crystallographic data for compound 2 has been published previously.<sup>[25]</sup>

**Synthesis of 3:** Compound 1 (0.75 g, 0.72 mmol) and 1-pyridin-3-yl-3-*p*-tolylurea (1.31 g, 5.77 mmol) were dissolved in ethanol (340 mL) and stirred at reflux for 44 h. During this time, a brown precipitate was formed and stuck to the round-bottomed flask. The reaction mixture was filtered to remove any of the brown solid. The solution was concentrated by removing ethanol (290 mL) under reduced pressure. The observed precipitate was filtered. The resultant precipitate was sticky and was not fully characterised. The precipitate was dissolved in methanol (50 mL) with NH<sub>4</sub>PF<sub>6</sub> (10 equiv, 1.17 g, 7.22 mmol) and stirred at ambient temperature for 6 h. A pale orange precipitate of 1,1'-bis(2,4,6-triethyl-3,5-bis[[3-(3-*p*-tolylureido)pyridinium-1-yl]benzyl])-4,4'-bipyridine-1,1'-dium hexafluorophosphate was observed, which was recovered by filtration and dried under ambient conditions (0.44 g, 0.19 mmol, 31 %). M.p. 206–213 °C dec; <sup>1</sup>H NMR (CD<sub>3</sub>CN, 400 MHz): δ = 8.97 (s, 4H; PyH), 8.95 (brs, 4H; NH), 8.62 (d, *J* = 6.6 Hz, 4H; *Hobipy*), 8.51 (d, *J* = 6.8 Hz, 4H; PyH), 8.26 (s, 4H; NH), 7.97 (d, *J* = 8.4 Hz, 4H; PyH), 7.92 (dd, *J* = 9.0, 5.9 Hz, 4H; PyH), 7.65 (d, *J* = 6.6 Hz, 4H; *Hmbipy*), 7.04 (d, *J* = 8.1 Hz, 8H; ArH), 6.79 (d, *J* = 8.1 Hz, 8H; ArH), 5.96 (s, 4H; -CH<sub>2</sub>-Py<sup>+</sup>), 5.92 (s, 8H; -CH<sub>2</sub>-Py<sup>+</sup>), 2.79 (q, *J* = 7.4 Hz, 4H; -CH<sub>2</sub>CH<sub>3</sub>), 2.53 (brs, 8H; -CH<sub>2</sub>CH<sub>3</sub>), 2.08 (brs, 12H; -CH<sub>3</sub>), 1.29 (t, *J* = 7.4 Hz, 6H; -CH<sub>2</sub>CH<sub>3</sub>), 1.22 ppm (t, *J* = 7.5 Hz, 12H; -CH<sub>2</sub>CH<sub>3</sub>); <sup>13</sup>C{<sup>1</sup>H} NMR (CD<sub>3</sub>CN, 100 MHz): δ = 206.5, 152.4, 152.0, 151.4, 149.6, 144.8, 141.4, 137.5, 135.6, 133.8, 133.4, 132.0, 129.6, 128.6, 128.4, 127.3, 120.0, 58.4, 58.1, 24.5, 24.3, 20.0, 15.1, 14.8 ppm; IR: ν̄ = 3413 (s, N-H), 3120 (m, Ar C-H), 2983 (m, CH<sub>2</sub>/CH<sub>3</sub>), 1714, 1636 (s, ArC=C), 1593 (s, urea C=O), 1551 (s, Ar C=C), 1503 (s, Ar C=C), 1460, 1443, 1408 (m, CH<sub>2</sub>/CH<sub>3</sub> def), 1390 (w, CH<sub>3</sub> def), 1315, 1295, 1243, 840 cm<sup>-1</sup>; MS (ES<sup>+</sup>): *m/z*: 1024 [M-2(PF<sub>6</sub>)]<sup>2+</sup>, 748, 732, 634 [M-3(PF<sub>6</sub>)]<sup>3+</sup>, 569, 478, 337, 227 [TUP]<sup>+</sup>, 183 [C<sub>12</sub>H<sub>11</sub>N<sub>2</sub>]<sup>+</sup>, 174, 129 (TUP = 3-*p*-tolylureidopyridinium); elemental analysis calcd (%) for C<sub>92</sub>H<sub>102</sub>N<sub>14</sub>P<sub>6</sub>F<sub>36</sub>: C 47.27, H 4.40, N 8.39; found: C 47.36, H 4.56, N 8.23.

**Synthesis of 4:** Compound 1 (0.50 g, 0.45 mmol) and *N*-(naphthalene-1-yl)methylpyridine-3-amine<sup>[27]</sup> (0.45 g, 1.93 mmol) were placed in a 25 mL grinding jar with 5 drops of acetonitrile. The reactants were ground at 18 Hz for 60 min after which methanol was added and any unreacted starting material was removed by filtration. Excess NH<sub>4</sub>PF<sub>6</sub> (approximately 10 equiv) was added to the methanol solution and the product precipitated as the PF<sub>6</sub><sup>-</sup> salt. The compound was recrystallised from acetonitrile/diethyl ether (0.446 g, 0.19 mmol, 39 %). M.p. 250 °C dec; <sup>1</sup>H NMR (CD<sub>3</sub>CN, 700 MHz): δ = 8.78 (s, 4H; ArH), 8.36 (d, *J* = 7.0 Hz, 4H; ArH), 8.05 (d, *J* = 8.1 Hz, 4H; ArH), 7.97 (d, *J* = 7.6 Hz, 4H; ArH), 7.87 (m, 8H; ArH), 7.60 (m, 10H; ArH), 7.45 (m, 8H; ArH), 6.40 (brs, 4H; NH), 5.87 (s, 4H; CH<sub>2</sub>), 5.62 (s, 8H; CH<sub>2</sub>-Py<sup>+</sup>), 4.88 (d, *J* = 5.5 Hz, 8H; CH<sub>2</sub>CH<sub>3</sub>), 2.53 (q, *J* = 7.6 Hz, 8H; CH<sub>2</sub>CH<sub>3</sub>), 2.48 (q, *J* = 7.6 Hz, 12H; CH<sub>2</sub>CH<sub>3</sub>), 0.91 (brs, 12H; CH<sub>3</sub>), 0.85 ppm (brs, 24H; CH<sub>3</sub>); <sup>13</sup>C{<sup>1</sup>H} NMR (CD<sub>3</sub>CN, 176 MHz): δ = 150.5, 148.2, 144.7, 133.9, 131.6, 131.1, 130.3, 128.8, 128.4, 128.1, 128.1, 127.5, 126.7, 126.5, 126.2, 125.5, 125.0, 123.2, 58.1, 57.5, 44.5, 23.8, 23.7, 14.3, 14.0 ppm; IR: ν̄ = 3431 (w, N-H), 3070 (w, C-H), 2983 (w, CH<sub>2</sub>/CH<sub>3</sub>), 1636 (m, Ar C=C), 1504 (w, Ar C=C), 1446 (m, Ar C=C), 1150, 1041, 823 cm<sup>-1</sup>; elemental analysis calcd (%) for C<sub>104</sub>H<sub>106</sub>F<sub>36</sub>N<sub>10</sub>P<sub>6</sub>·8H<sub>2</sub>O: C 49.77, H 4.90, N 5.58; found: C 49.49, H 4.36, N 5.55. Reliable mass spectrometry data could not be obtained for this compound.

**Synthesis of 5:** 1,3,5-Tri(bromomethyl)-2,4,6-triethylbenzene (0.50 g, 1.1 mmol) and 4,4'-bipyridine (1.77 g, 11.3 mmol) were dissolved in dry dichloromethane (150 mL). The resulting solution was stirred at reflux under N<sub>2</sub> for 23 h. A pale yellow precipitate was produced and isolated by filtration (0.97 g, 1.07 mmol, 95 %). Characterisation data was consistent with those published in the literature.<sup>[24]</sup>

**Synthesis of 6:** 1,3,5-Tris(4-bipyridinium)-2,4,6-triethylbenzene tribromide (0.38 g, 0.41 mmol) was dissolved in dry DMF (5 mL). Then benzyl bromide (0.52 mL, 4.38 mmol) was added and the yellow mixture was allowed to stir at 70 °C for 20 h under N<sub>2</sub>. During the reaction a yellow-brownish precipitate occurred. After cooling, the mixture was poured into diethyl ether and a yellow precipitate was observed and it was isolated by filtration. During drying the product became a sticky brown oil and therefore was metathesised to the PF<sub>6</sub> salt immediately by dissolving

in methanol and addition of excess  $\text{NH}_4\text{PF}_6$  (approximately 10 equiv, 1.5 g), without characterisation of the bromide salt to give a white powder (0.53 g, 0.30 mmol, 71%). M.p. 250°C dec;  $^1\text{H}$  NMR ( $\text{CD}_3\text{CN}$ , 700 MHz):  $\delta$  = 8.96 (d,  $J$  = 7.0 Hz, 8H; bipy-H), 8.92 (d,  $J$  = 6.9 Hz, 8H; bipy-H), 8.40 (d,  $J$  = 7.0 Hz, 8H; bipy-H), 8.36 (d,  $J$  = 6.9 Hz, 8H; bipy-H), 7.51 (s, 15H; Ph), 6.00 (s, 6H;  $\text{CH}_2\text{-Py}^+$ ), 5.82 (s, 6H;  $\text{CH}_2\text{-Py}^+$ ), 2.60 (q,  $J$  = 7.3 Hz, 6H;  $\text{CH}_2\text{CH}_3$ ), 1.09 ppm (t,  $J$  = 7.3 Hz, 9H;  $\text{CH}_3$ );  $^{13}\text{C}$  ( $^1\text{H}$ ) NMR ( $\text{CD}_3\text{CN}$ , 176 MHz):  $\delta$  = 152.5, 151.5, 151.4, 146.6, 145.8, 133.5, 131.1, 130.6, 130.3, 128.5, 65.8, 59.1, 25.0, 15.5 ppm; IR:  $\tilde{\nu}$  = 3131 (w, C-H), 3069 (w, C-H), 1637 (m, Ar C=C), 1561 (w, Ar, C=C), 1499 (w, Ar, C=C), 1447 (m, Ar, C=C), 1220, 1144, 1002, 823  $\text{cm}^{-1}$ ; MS (MALDI $^+$ ):  $m/z$ : 563.2, 565.2, 647.5, 649.5, 663.5, 1667.3 [ $M\text{-PF}_6$ ] $^+$ ; elemental analysis calcd (%) for  $\text{C}_{66}\text{H}_{66}\text{F}_{36}\text{N}_6\text{P}_6\cdot 4\text{H}_2\text{O}$ : C 42.05, H 3.96, N 4.46; found: C 41.98, H 3.62, N 4.55.

## Acknowledgements

We are grateful to Durham University and the EPSRC for funding (to A.N.S. and S.J.D, respectively), the Heriot-Watt University Information and Computing Services for use of the Heriot-Watt high-performance cluster service, Dr. Ian Terry (Dept. Physics, Durham University) for ESR measurements and Lucas Applegarth for assistance with Raman spectroscopy.

- [1] J. L. Sessler, P. A. Gale, W.-S. Cho, *Anion Receptor Chemistry*, RSC, Cambridge, **2006**.
- [2] C. Caltagirone, P. A. Gale, *Chem. Soc. Rev.* **2009**, 38, 520.
- [3] P. A. Gale, *Coord. Chem. Rev.* **2006**, 250, 2917 preface to the special issue and subsequent reviews.
- [4] T. Gunnlaugsson, M. Glynn, G. M. Tocci, P. E. Kruger, F. M. Pfeffer, *Coord. Chem. Rev.* **2006**, 250, 3094.
- [5] M. H. Filby, T. D. Humphries, D. R. Turner, R. Katak, J. Kruusma, J. W. Steed, *Chem. Commun.* **2006**, 156.
- [6] M. Boiocchi, L. Del Boca, D. Esteban-Gomez, L. Fabbrizzi, M. Licchelli, E. Monzani, *Chem. Eur. J.* **2005**, 11, 3097.
- [7] V. Amendola, D. Esteban-Gomez, L. Fabbrizzi, M. Licchelli, *Acc. Chem. Res.* **2006**, 39, 343.
- [8] K. J. Wallace, W. J. Belcher, D. R. Turner, K. F. Syed, J. W. Steed, *J. Am. Chem. Soc.* **2003**, 125, 9699.
- [9] D. R. Turner, M. J. Paterson, J. W. Steed, *J. Org. Chem.* **2006**, 71, 1598.
- [10] M. H. Filby, S. J. Dickson, N. Zacheroni, L. Prodi, S. Bonacchi, M. Montalti, C. Chiorboli, M. J. Paterson, T. D. Humphries, J. W. Steed, *J. Am. Chem. Soc.* **2008**, 130, 4105.
- [11] V. Amendola, M. Boiocchi, L. Fabbrizzi, A. Palchetti, *Chem. Eur. J.* **2005**, 11, 5648.
- [12] H. Ihm, S. Yun, H. G. Kim, J. K. Kim, K. S. Kim, *Org. Lett.* **2002**, 4, 2897.
- [13] Y. Bai, B. G. Zhang, J. Xu, C. Y. Duan, D. B. Dang, D. J. Liu, Q. J. Meng, *New J. Chem.* **2005**, 29, 777.
- [14] Y. Bai, B.-G. Zhang, C. Y. Duan, D.-B. Dang, Q.-J. Meng, *New J. Chem.* **2006**, 30, 266.
- [15] L. O. Abouderbala, W. J. Belcher, M. G. Boutelle, P. J. Cragg, M. Fabre, J. Dhaliwal, J. W. Steed, D. R. Turner, K. J. Wallace, *Chem. Commun.* **2002**, 358.
- [16] A. Metzger, V. M. Lynch, E. V. Anslyn, *Angew. Chem.* **1997**, 109, 911; *Angew. Chem. Int. Ed. Engl.* **1997**, 36, 862.
- [17] G. Hennrich, E. V. Anslyn, *Chem. Eur. J.* **2002**, 8, 2218.
- [18] J. W. Steed, *Chem. Commun.* **2006**, 2637.
- [19] G. Rogez, B. F. Ribera, A. Credi, R. Ballardini, M. T. Gandolfi, V. Balzani, Y. Liu, B. H. Northrop, J. F. Stoddart, *J. Am. Chem. Soc.* **2007**, 129, 4633.
- [20] W. Sliwa, B. Bachowska, T. Girek, *Curr. Org. Chem.* **2007**, 11, 497.
- [21] M. Ezoe, S. Yagi, H. Nakazumi, M. Itou, Y. Araki, O. Ito, *Tetrahedron* **2006**, 62, 2501.
- [22] S. P. Gromov, A. I. Vedernikov, E. N. Ushakov, N. A. Lobova, A. A. Botsmanova, L. G. Kuz'mina, A. V. Churakov, Y. A. Strelenko, M. V. Alfimov, J. A. K. Howard, D. Johnels, U. G. Edlund, *New J. Chem.* **2005**, 29, 881.
- [23] P. M. S. Monk, *The Viologens: Physicochemical Properties Synthesis and Applications of the Salts of 4,4'-Bipyridine*, Wiley, New York, **1998**.
- [24] W. J. Belcher, M. Fabre, T. Farhan, J. W. Steed, *Org. Biomol. Chem.* **2006**, 4, 781.
- [25] S. J. Dickson, E. V. B. Wallace, A. N. Swinburne, M. J. Paterson, G. O. Lloyd, A. Beeby, J. W. Steed, *New J. Chem.* **2008**, 32, 786.
- [26] D. R. Turner, E. C. Spencer, J. A. K. Howard, D. A. Tocher, J. W. Steed, *Chem. Commun.* **2004**, 1352.
- [27] A. N. Swinburne, J. W. Steed, *CrystEngComm* **2009**, 11, 433.
- [28] P. Gans, *HypNMR 2006*, University of Leeds, Leeds, **2006**.
- [29] P. M. S. Monk, N. M. Hodgkinson, *Electrochim. Acta* **1998**, 43, 245.
- [30] P. M. S. Monk, N. M. Hodgkinson, R. D. Partridge, *Dyes Pigm.* **1999**, 43, 241.
- [31] S. G. Bertolotti, J. J. Cosa, H. E. Gsponer, C. M. Previtali, *Can. J. Chem.* **1987**, 65, 2425.
- [32] S. M. Hubig, J. K. Kochi, *J. Phys. Chem.* **1995**, 99, 17578.
- [33] G. Briegleb, J. Czekalla, *Z. Elektrochem.* **1959**, 63, 6.
- [34] B. G. White, *Trans. Faraday Soc.* **1969**, 65, 2000.
- [35] A. Ledwith, H. J. Woods, *J. Chem. Soc. C* **1970**, 1422.
- [36] A. S. N. Murthy, A. P. Bhardwaj, *Spectrochim. Acta Part A* **1982**, 38, 207.
- [37] J. P. Kuczynski, B. H. Milosavljevic, A. G. Lappin, J. K. Thomas, *Chem. Phys. Lett.* **1984**, 104, 149.
- [38] T. M. Bockman, J. K. Kochi, *J. Org. Chem.* **1990**, 55, 4127.
- [39] C. L. Bird, A. T. Kuhn, *Chem. Soc. Rev.* **1981**, 10, 49.
- [40] S. Hünig, W. Schenk, *Liebigs Ann. Chem.* **1979**, 1523.
- [41] M. Arroyo, P. R. Birkin, P. A. Gale, S. E. Garcia-Garrido, M. E. Light, *New J. Chem.* **2008**, 32, 1221.
- [42] F. Ito, T. Nagamura, *J. Photochem. Photobiol. C* **2007**, 8, 174.
- [43] C. S. Johnson, H. S. Gutowsky, *J. Chem. Phys.* **1963**, 39, 58.
- [44] M. Forster, R. B. Girling, R. E. Hester, *J. Raman Spectrosc.* **1982**, 12, 36.
- [45] C. A. Melendres, P. C. Lee, D. Meisel, *J. Electrochem. Soc.* **1983**, 130, 1523.
- [46] D. J. Barker, R. P. Cooney, L. A. Summers, *J. Raman Spectrosc.* **1987**, 18, 443.
- [47] Y. X. Huang, J. B. Hopkins, *J. Phys. Chem.* **1996**, 100, 9585.
- [48] N. G. Connelly, W. E. Geiger, *Chem. Rev.* **1996**, 96, 877.
- [49] K. J. Wallace, R. Hanes, E. Anslyn, J. Morey, K. V. Kilway, J. Siegel, *Synthesis* **2005**, 2080.

Received: September 22, 2009  
Published online: December 18, 2009